Gene Therapy (2013) **20,** 487–496

www.nature.com/gt

ORIGINAL ARTICLE

Lentiviral-mediated administration of IL-25 in the CNS induces alternative activation of microglia

C Maiorino[1], R Khorooshi[2], F Ruffini[1], M Løbner[2], A Bergami[1], L Garzetti[1], G Martino[3], T Owens[2] and R Furlan[1]

Interleukin-25 (IL-25) is the only anti-inflammatory cytokine of the IL-17 family, and it has been shown to be efficacious in inhibiting neuroinflammation. Known for its effects on cells of the adaptive immune system, it has been more recently described to be effective also on cells of the innate immune system, namely macrophages. We used a lentiviral-mediated gene therapy approach to deliver IL-25 to the central nervous system (CNS) in two mouse models of neuroinflammation, entorhinal cortex lesion and experimental autoimmune encephalomyelitis. In both, we found that IL-25 gene therapy was able to modulate CNS myeloid cells, either infiltrating macrophages or resident microglia, towards an anti-inflammatory, tissue-protective phenotype, as testified by the increase in markers such as Arginase-1 (Arg1), Mannose receptor 1 (CD206) and Chitinase 3-like 3 (Ym1). As a consequence, neuroinflammation was partly inhibited and the CNS protected from immune-mediated damage. To our knowledge, this is the first example of M2 shift (alternative activation) induced *in vivo* on CNS-resident myeloid cells by gene therapy, and may constitute a promising strategy to investigate the potential role of protective microglia in neurological disorders.

Gene Therapy (2013) **20,** 487–496; doi:10.1038/gt.2012.58; published online 2 August 2012

Keywords: IL-25; microglia; M1/M2; autoimmunity; EAE; neuroinflammation

INTRODUCTION

Interleukin-25 (IL-25), also known as IL-17e, is the only member of the IL-17 cytokine family that exerts anti-inflammatory properties.[1] Produced by several cells, such as Type 2 helper T (Th2) cells, mast cells, epithelial cells, eosinophils, basophils and alveolar macrophages,[2–6] IL-25 was initially described to modulate Th2 cell function in autoimmune disorders and type 2-cytokine immune diseases,[7–10] underlining its function in adaptive immune responses. However, recent studies suggest a new role for IL-25 on cells of the innate immune system, for example macrophages.[11–14] IL-25, in fact, protects mice from colitis and proteinuric kidney disease by promoting alternative (M2) macrophage activation and thus inhibiting inflammation *in vivo*,[11,14] a finding not paralleled by corresponding *in vitro* data.[15,16]

Despite being extremely plastic in the activation phenotype they can display, macrophages polarize towards two main functional phenotypes, according to activation stimuli.[17–19] Classical Toll-like receptor agonists, that is, lipopolysaccharide, or pro-inflammatory cytokines, induce a phagocytic, pro-inflammatory (M1) activation state, characterized by the production of IL-1β, tumor necrosis factor alpha (TNFα), inducible nitric oxide synthases (iNOS) and reactive oxygen species;[20,21] while IL-4 induces alternative (M2) activation, characterized by anti-inflammatory and tissue-remodeling functions and the expression of markers such as Arginase-1 (Arg-1), Chitinase 3-like 3 (Ym1), mannose receptor 1 (CD206) and CC chemokine ligand 17 and 22 (CCL17 and CCL22).[22–25]

Microglia are the resident macrophages of the central nervous system (CNS) whose activation is considered a pathological hallmark of several neurodegenerative disorders, such as multiple sclerosis.[20,26] The M1/M2 paradigm, validated for macrophages, has not really been explored in detail for microglia. However, several lines of evidence suggest that microglia display functional phenotypes that are similar to peripheral macrophages.[27–30] As pro-inflammatory microglia are considered crucial in the vicious circle leading to neuronal death in classical neurodegenerative disorders, and in the progressive phases of MS, both still lacking efficacious treatment, it is commonly believed that modulation of microglia towards a protective phenotype might be a useful therapeutic strategy for these disorders.[31–35]

IL-25 has been shown previously to inhibit neuroinflammation[9], and the aim of the present work has been to investigate if IL-25 modulates microglia inducing an anti-inflammatory, protective phenotype. We took advantage of the common previous pioneering experience of our groups in delivering cytokines to the CNS using the so called 'ependymal route'.[36] Briefly, lentiviral vectors engineered to express cytokines are injected in cerebrospinal fluid spaces, infecting ependymal and leptomeningeal cells that, in turn, produce and release the desired cytokine into the cerebrospinal fluid (CSF), thus reaching the entire CNS.[37–42] Using this gene therapy approach, after *in vitro* validation of the IL-25-expressing lentiviral vector, we administered IL-25 in two mouse models of neuroinflammation, the entorhinal cortex lesion (ECL) model[43–46] and experimental autoimmune encephalomyelitis (EAE).[47] We found that IL-25 was indeed able to shift CNS myeloid cells towards an anti-inflammatory phenotype and to inhibit neuroinflammation. This approach to modulate microglia may therefore be useful to investigate their role in physiology and pathology, and constitute an alternative therapeutic approach in diseases where microglia are considered crucial.

[1]Clinical Neuroimmunology Unit, Institute of Experimental Neurology-INSpe, Division of Neuroscience, San Raffaele Scientific Institute, Milan, Italy; [2]Neurobiology Research, Institute of Molecular Medicine, University of Southern Denmark, Odense, Denmark and [3]Neuroimmunology Unit, Institute of Experimental Neurology–INSpe, Division of Neuroscience, San Raffaele Scientific Institute, Milan, Italy. Correspondence: Dr R Furlan, Clinical Neuroimmunology Unit, Institute of Experimental Neurology-INSpe, Division of Neuroscience, San Raffaele Scientific Institute, Via Olgettina 58, 20132 Milan, Italy.
E-mail: furlan.roberto@hsr.it

This work has been supported by FISM (RF), Danish Agency for Science, Technology and Innovation (TO), Lundbeck Foundation (ML) and MSIF Du Pré Grant Fellow (CM). CM conducted this study as partial fulfillment of her PhD in Molecular Medicine, Program in Experimental Neurology, San Raffaele University, Milan, Italy.
Received 27 January 2012; revised 7 June 2012; accepted 8 June 2012; published online 2 August 2012

RESULTS

IL-25 inhibits M1 and M2 cytokine expression in myeloid cells *in vitro*

We constructed a third-generation lentiviral vector by cloning murine IL-25, modified to carry a hemagglutinin epitope as a tag (HA-tag) at the C-terminus (IL-25HA), downstream of a human phosphoglycerate kinase promoter. We found that the supernatant of infected HEK293T cells contained high amounts of tagged IL-25HA (Figure 1a), detected also by an enzyme-linked immunosorbent assay (ELISA) for mouse IL-25 (Supplementary Figure 1a). We next ascertained that myeloid cells, in this case bone marrow (BM)-derived macrophages, express IL-17rb, the IL-25 receptor, as shown by confocal fluorescent microscopy in Figure 1b and by fluorescence-activated cell sorting (FACS) staining (data not shown). Finally, we confirmed that IL-25HA activates the appropriate signaling pathway in BM-macrophages by inducing p38 phosphorylation, comparable to recombinant IL-25 (rIL-25) (Supplementary Figure 1b), and by inducing expression of IL-4, IL-5 and IL-13 messenger RNA (mRNA) in spleenocytes (Figure 1c), as previously described.[48]

After validation of our construct in terms of expression and bioactivity, we next examined its effects on myeloid cells. IL-25HA administered to purified BM-macrophages in culture induced a decrease in the mRNA expression of both M1 (IL-1β and TNF-α) and M2 (CD206) activation markers, together with T-cell-attracting chemokines (CCL2 and CXCL10) and a significant increase of Socs3 mRNA expression, similar to rIL-25 (Figure 1d).

IL-25 gene therapy induces alternative activation of microglia in an ECL model

We next verified if IL-25 was able to inhibit microglia activation *in vivo* similar to macrophages *in vitro*. We therefore investigated the effects of IL-25HA, delivered by lentiviral gene therapy, on microglia in the ECL mouse model. In this model, microglia become activated in response to synaptic degeneration following transection of perforant path (PP) axons in the entorhinal cortex[43] (Figure 2a). The IL-25HA-expressing lentivirus (lenti-IL-25HA) was delivered by intracisternal (i.c.) injection 5 days before the PP lesioning, as previously described. At 48 h post transection, thus 7 days post lentiviral infection, ependymal and leptomeningeal cells close to the hippocampus, where microglia activation occurs, are infected by this procedure (Figure 2b). Moreover, we detected efficient IL-25HA mRNA transcription in hippocampi of mice injected with Lenti-IL-25HA (Figure 2c).

To investigate the functional significance of IL-25 in ECL model, 5 days before PP-axons transection, C57Bl/6 mice were i.c. injected with lenti-IL-25HA or green fluorescent protein (GFP)-expressing lentivirus and killed 48 h post surgical lesion for FACS, real-time reverse transcriptase PCR (RT-PCR)

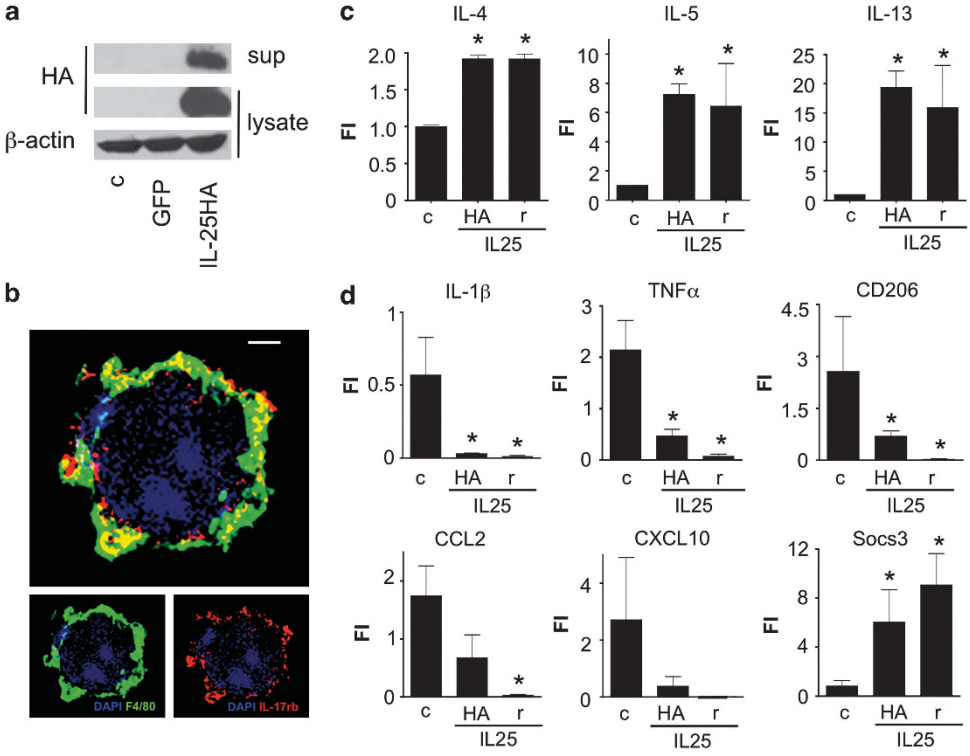

Figure 1. IL-25 inhibits both M1 and M2 cytokine expression in myeloid cells *in vitro*. (**a**) HEK293T cells infected with the lentiviral vector expressing IL-25HA (IL-25HA) produce the IL-25HA protein (lysate) and release it in the supernatant (sup) 48 h after infection, as shown by western blot analysis for the HA-tag (HA). Cells infected with a GFP-expressing lentiviral vector (GFP) or uninfected cells (c) were used as negative control; β-actin was used as normalizer. (**b**) BM-derived macrophages express IL-17rb, as shown by immunofluorescence for IL-17rb (red) and F4/80 (green); single staining (lower panels) are also shown. Original magnification ×63, scale bar = 2 μm. (**c**) IL-25HA-conditioned medium (ratio 1:1) induces overexpression of IL-4, IL-5 and IL-13 in spleen cells after 48 h of incubation, as shown by real-time (RT)-PCR analysis. GFP-conditioned medium (c, ratio 1:1) or rIL-25 (50 ng ml^{-1}) were used as controls. (**d**) RT-PCR analysis of IL-1β, TNF-α, CD206, CCL2, CXCL10 and Socs3 mRNA transcripts of BM-macrophages incubated with GFP-conditioned medium (c, in a ratio 1:1 to α-MEM), IL-25HA-conditioned medium (HA, in a ratio 1:1 to α-MEM) or rIL-25 (r, 50ng ml^{-1}) for 48 h. IL-25 inhibits both M1 and M2 cytokine expression when added to BM-macrophages. For RT-PCR studies, gene expression values were shown as mRNA expression fold increase (FI) and were normalized on the glyceraldehyde-3-phosphate dehydrogenase housekeeping gene. The average of RT-PCR results from three different experiments are shown (**c**, **d**). In (**a**), c = uninfected cells, GFP = GFP-infected cells, IL-25HA = IL-25HA-infected cells. In (**c**, **d**) c = GFP-conditioned medium, HA = IL-25HA-conditiond medium, r = rIL-25. *$P < 0.05$, significance is lost after Bonferroni's correction for multiple comparison.

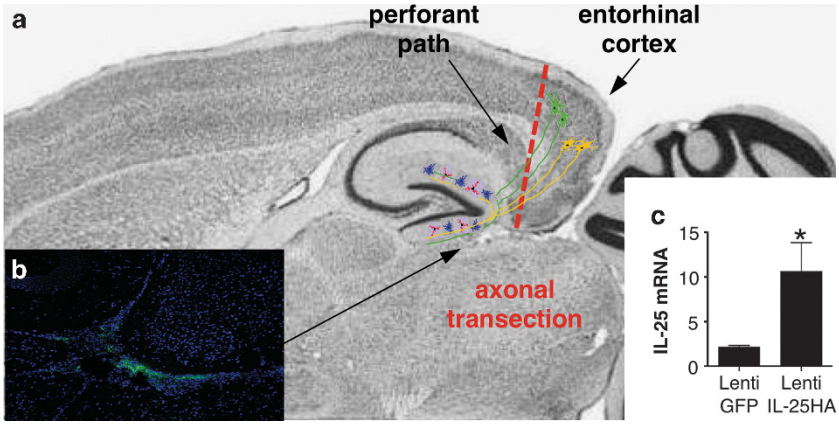

Figure 2. IL-25 gene therapy in the mouse model of ECL. (**a**) Representative scheme of the ECL in a mouse brain (axial brain section is shown): the surgical transection (axonal transection) of PP axons (neurons are drawn in green and yellow) of entorhinal cortex causes glial activation (activated microglia and astrocytes are drawn in blue and red) in the outer molecular layer of the dentate gyrus in the injured hemisphere. (**b**) Immunofluorescence staining for HA-tag of a PP-injured IL-25HA-injected brain: ependymal- and leptomeningeal-infected cells can be found 7 days post *intra cisterna magna* (i.c.) injection of the IL-25HA-expressing lentivirus. (**c**) IL-25HA-lentivirus injection induces a dramatic increase in IL-25 mRNA expression in hippocampi ($n=6$, Lenti-IL-25HA) as compared with GFP-injected mice ($n=5$, Lenti-GFP) 7 days post i.c. as shown by real-time (RT)-PCR analysis; gene expression values were normalized on the glyceraldehyde-3-phosphate dehydrogenase housekeeping gene. Column bars represent mean FI and s.e.m. $^*P<0.05$.

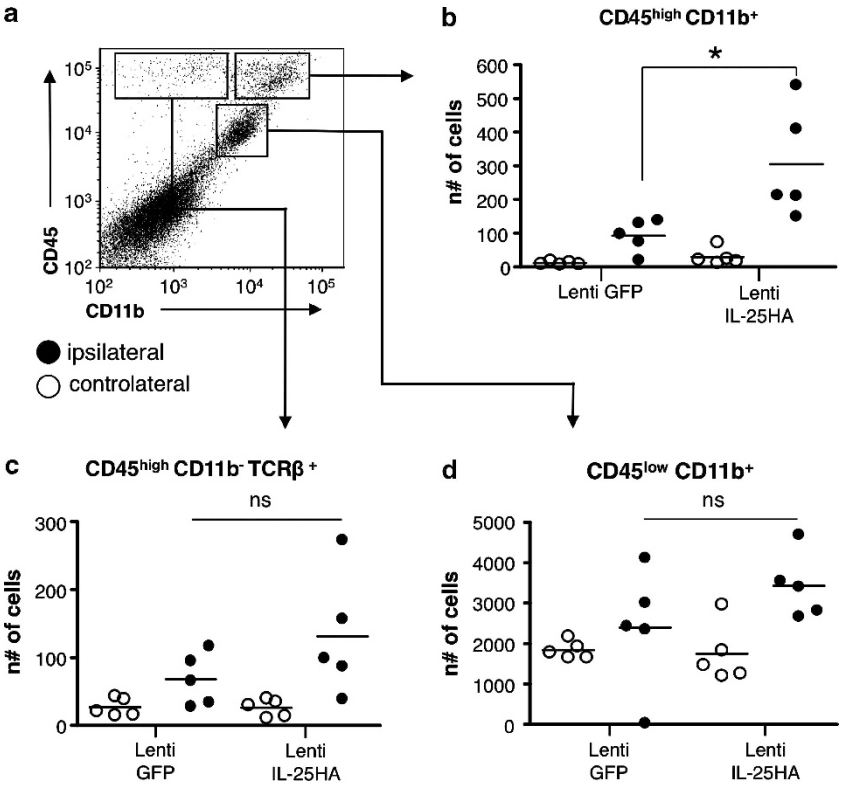

Figure 3. IL-25 gene delivery induces an increase of $CD45^{high}/CD11b^+$ myeloid cells *in vivo*. (**a**) Representative dot plot of flow cytometry analysis of brain cells stained for CD11b and CD45, 48 hours post axonal transection. (**b**) IL-25 treatment promotes an increase in the number of $CD45^{high}/CD11b^+$ activated myeloid cells in the lesioned hippocampi ($n=5$, ipsilateral) in comparison with GFP-injected ipsilateral hippocampi ($n=5$); $^*P<0.05$. No differences in the number of $CD45^{high}/CD11b^-/TCR\beta^+$ T cells (**c**) or $CD45^{low}/CD11b^+$ microglia (**d**) were observed. Lenti-GFP, PP-injured GFP-injected mice, Lenti-IL-25HA, PP-injured IL-25HA-injected mice; black dots, ipsilateral hippocampus values and white dots, controlateral hippocampus values. Horizontal bars represent mean values. NS, not significant.

or histological analysis. When we measured the number of infiltrating $CD45^+CD11b^+$ myeloid cells to the lesion-reactive hippocampi (Figure 3), we found, as expected, that synaptic degeneration induced an increase in the number of infiltrating $CD45^{high}CD11b^+$ myeloid cells to the lesion-reactive hippocampi of both lenti-GFP-injected control mice and lenti-IL-25HA-injected mice. However, the number of infiltrating $CD45^{high}CD11b^+$ myeloid cells were significantly higher in the lesion-reactive

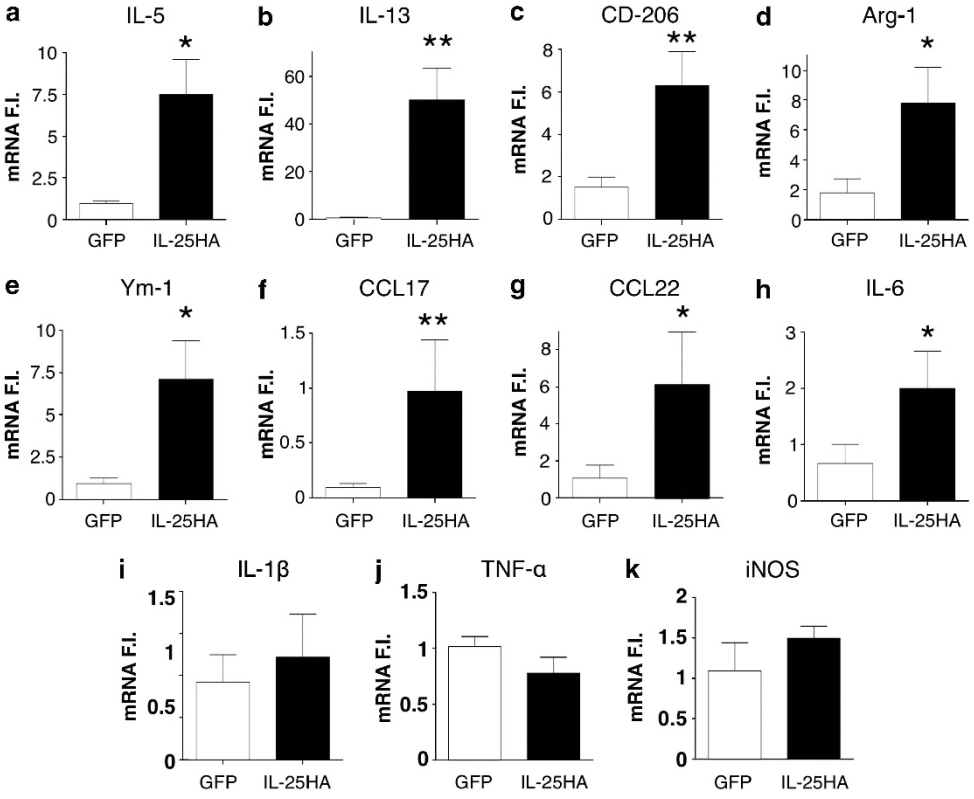

Figure 4. IL-25 promotes M2 alternative activation of microglia *in vivo*. Real-time (RT)-PCR analysis of perforant-path (PP)-injured hippocampi in IL-25HA-injected ($n = 6$) versus GFP-injected mice ($n = 5$). Graphs show the mRNA expression FI of IL-5 (**a**), IL-13 (**b**), CD206 (**c**), Arg-1 (**d**), Ym1 (**e**), CCL17 (**f**), CCL22 (**g**), IL-6 (**h**), IL-1β (**i**), TNF-α (**j**) and iNOS (**k**); gene expression values were normalized on the glyceraldehyde-3-phosphate dehydrogenase housekeeping gene. Column bars represent mean FI with s.e.m. $^{*}P < 0.05$; $^{**}P < 0.01$. One asterisk significance is lost after Bonferroni's correction for multiple comparison. Lenti-GFP = PP-injured GFP-injected mice, Lenti-IL-25HA = PP-injured IL-25HA-injected mice.

hippocampi of mice injected with IL-25HA than in control mice (Figure 3b). In contrast, IL-25 had no effect on the number of $CD45^{low}CD11b^{+}$ microglia or on the synaptic degeneration-induced increase in $CD45^{high}CD11b^{-}TCR\beta^{+}$ T cells as compared with control mice (Figures 3c–d).

RT-PCR analysis conducted on whole hippocampi showed that, IL-25 induces IL-5 and IL-13 anti-inflammatory cytokines mRNA expression (Figures 4a–c), as previously demonstrated in *in vitro* assay. However, in distinction from isolated myeloid cell cultures, M2 activation markers (that is, CD206, Arg-1, YM-1, CCL17 and CCL22; Figures 4c–g) and, surprisingly, IL-6 (Figure 4h) were markedly increased, while M1 activation markers were unaffected (that is, IL-1β, TNF-α and iNOS; Figures 4g–i). Sorting and individual phenotype analysis was not possible owing to the low number of cells isolated from hippocampi. However, we analyzed by confocal microscopy the expression of the M2 marker mannose receptor 1 (CD206) that was increased by RT-PCR, and found it confined exclusively to microglia (Supplementary Figure 2). Compared with *in vitro* experiments, these data suggest that induction of M2 alternative activation of microglia *in vivo* is not dependent on IL-25 signaling in myeloid cells alone.

IL-25 gene therapy induces M2 markers during experimental neuroinflammation

Previous work had shown that IL-25 CNS gene therapy inhibits both chronic and relapsing EAE also when administered after disease onset.[9] Our i.c. IL-25HA-lentivirus injection approach, perfomed at 5 days post immunization (d.p.i.), very efficiently infects ependymal and leptomeningeal cells, also during acute neuroinflammation, as shown by immunohistochemistry analysis of 12 d.p.i. infected brain (Figure 5a) and induces very high levels of IL-25 protein in both the CSF and the CNS (Figure 5b). When we analyzed the effect of IL-25 gene therapy, we found inhibition in only chronic EAE when IL-25HA-expressing lentivirus was administered i.c. 5 d.p.i. (Figure 5c). Clinical amelioration of chronic EAE was associated to decreased tissue damage as measured by neuropathological analysis in terms of demyelination (Figure 5d and Supplementary Figures 4a and d) and axonal loss (Figure 5e and Supplementary Figures 4b and e).

Chronic EAE induced in C57BL/6 mice by immunization with MOG_{35-55} is characterized by a massive influx of inflammatory cells from the blood. In our studies, IL-25 gene therapy induced a significant decrease of inflammatory cells infiltration (Figure 5f and Supplementary Figures 4c and f) at 60 d.p.i. Moreover, FACS analysis for myeloid cells and T cells at 12 d.p.i. revealed that the number of infiltrating $CD45^{high}/CD11b^{+}$ myeloid cells and $CD45^{high}/CD11b^{-}/CD3^{+}$ T cells decreased in both brains and spinal cords of IL-25-treated EAE mice, compared with controls. The number of $CD45^{low}/CD11b^{+}$ microglia was reduced only in the spinal cord, where there is more inflammation (Figures 6a–d).

On the contrary, we found no effect of IL-25 gene therapy on relapsing remitting (RR)-EAE. IL-25HA gene delivery does not induce an amelioration of the disease when administered i.c. both on the twelth d.p.i. and on the eighteenth d.p.i., as shown in the clinical score graphs (Supplementary Figures 3a and c). No differences in the percentage of demyelinated areas or axonal damage or infiltrating cells number were reported for IL-25HA-injected, in both experiments (Supplementary Figures 3b and d, respectively; neuropathological analysis was performed at 50 d.p.i.).

Gene expression analysis on the CNS of EAE mice treated with IL-25 gene therapy reveals a very different scenario when

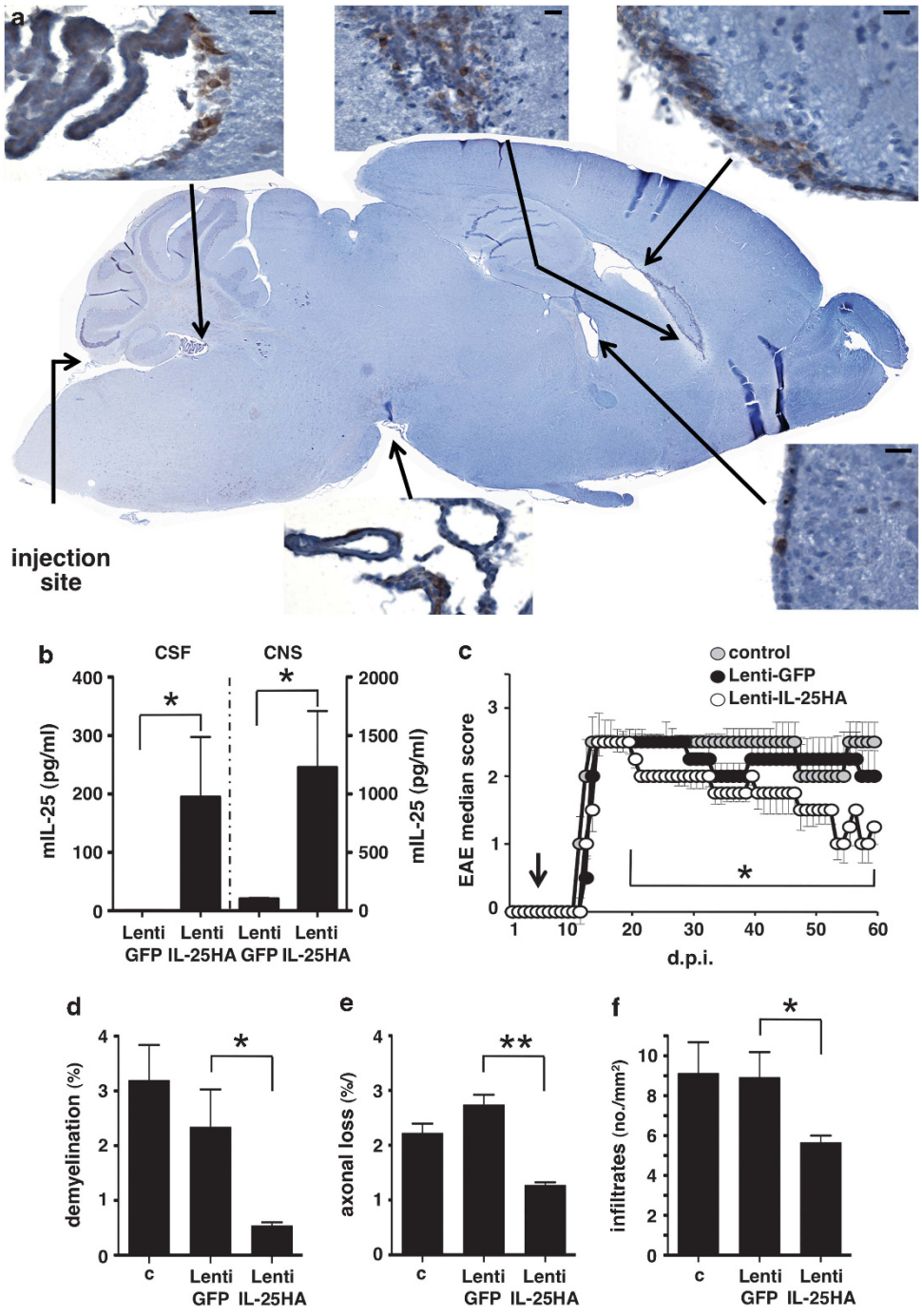

Figure 5. Preventive IL-25 gene therapy ameliorates chronic EAE. (**a**) HA-tag immunostaining of a sagittal brain section (× 4) of a IL-25HA-injected mouse at 12 d.p.i. reveals that i.c. injection of IL-25HA-expressing lentivirus allows infection of epedymal and leptomeningeal cells, from the injection site through all ventricular spaces (insets, × 40). Scale bars = 20 μm. (**b**) IL-25 production is increased in both CSFs and brain homogenates (CNS) of IL-25HA-injected EAE mice ($n = 5$) compared with GFP-injected EAE mice ($n = 5$) at 12 d.p.i., as shown by ELISA. Columns bars represent mean values with s.e.m.; *$P < 0.05$. (**c**) EAE median clinical score in IL-25HA-injected ($n = 8$, open dots) or GFP-injected ($n = 8$, closed dots) or uninjected ($n = 5$, gray dots) mice; lentiviruses i.c. injection was performed on the fifth d.p.i. (arrow). IL-25 preventive treatment ameliorates the chronic phase of EAE. Curves represents median score values with s.e.m. Difference between median clinical score of IL-25HA-injected versus GFP-injected EAE mice is significative starting from the twentieth d.p.i.; *$P < 0.05$. Neuropathological analysis reveals that clinical score amelioration in IL-25-treated mice ($n = 4$) associates with decreased infiltrating cells (**d**), myelin damage (**e**) and axonal loss (**f**) in comparison with GFP-treated mice ($n = 4$) or uninjected mice (c, $n = 2$) at 60 d.p.i. Column bars represent mean values with s.e.; *$P < 0.05$, **$P < 0.01$. c = uninjected EAE mice, Lenti-GFP = GFP-lentivirus-injected EAE mice, Lenti-IL-25HA = IL-25HA-lentivirus-injected EAE mice.

considered during the acute phase of the disease, when inflammation prevails, as compared with a very late stage of the disease, during the chronic phase of EAE. At 12 d.p.i., IL-25-treated EAE mice displayed a general inhibition of most markers tested, including Socs3 (not shown), with the notable exception of IL-4 that was increased (Figure 7). At 60 d.p.i., on the other hand, while chemoattractant chemokines and pro-inflammatory cytokines were still inhibited in IL-25 treatment, the anti-inflammatory

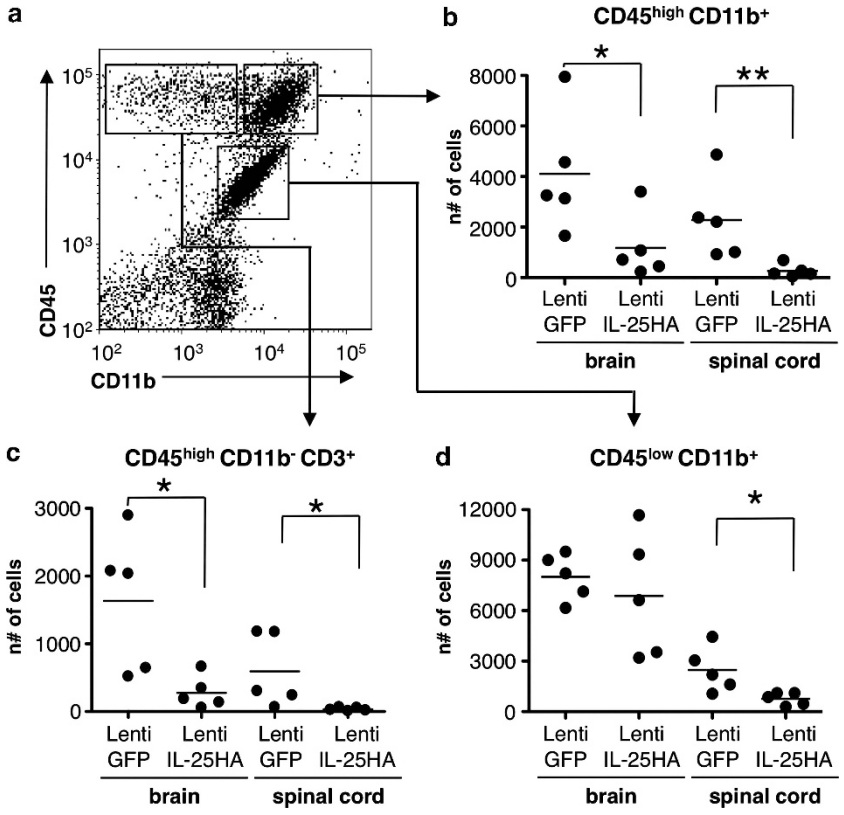

Figure 6. IL-25 treatment results in a decreased number of myeloid and T cells in EAE. (**a**) Representative dot plot of flow cytometry analysis of brain and spinal cord cells double stained for CD11b and CD45, isolated on the twelth d.p.i. IL-25 administration induces a significant decrease in the number of activated $CD45^{high}/CD11b^{+}$ myeloid cells (**b**) and in the number of $CD45^{high}/CD11b\text{-}/CD3^{+}$ T cells (**c**) in both brains and spinal cords of IL-25HA-injected EAE mice ($n = 5$) compared with GFP-injected EAE mice ($n = 5$). A slight decrease in the number of $CD45^{low}/CD11b^{+}$ microglia (**d**) is also observed only in the spinal cord. Lenti-GFP = GFP-lentivirus-injected mice, Lenti-IL-25HA = IL-25HA-lentivirus-injected mice. Horizontal bars represent mean values; $^{*}P < 0.05$, $^{**}P < 0.01$.

cytokines IL-5 and IL-13 and the M2 marker Arg-1 were significantly increased (Figure 7), suggesting again an alternatively activated phenotype induced by IL-25 gene therapy in CNS myeloid cells.

DISCUSSION

Currently, microglia are believed to have a crucial role in the pathogenesis of several neurological disorders. Translating to microglia the paradigm of pro-inflammatory (M1) or anti-inflammatory (M2) alternative activation, validated in peripheral macrophages, it has been hypothesized that in both neurodegeneration and the chronic phases of neuroinflammation alterations in activation state may have a pivotal role. Very little information, however, is available on the functional phenotype of microglia, whether detrimental (M1-like) or protective (M2-like), during human and experimental disease. This is owing to the difficulty in accessing microglia during human disease, and to purify these myeloid cells distinguishing them from infiltrating macrophages in animal models. Further, validated tools to modulate microglia response in one direction or the other *in vivo* are currently lacking. We believe we have shown here one of the very few successful examples of *in vivo* modulation of microglia to express markers associated to a protective M2 phenotype.

To this purpose, we exogenously expressed HA-tagged IL-25 from a lentiviral vector. IL-25 had been shown to be effective in neuroinflammation,[9] and we investigated the hypothesis that this beneficial effect might be mediated by microglia. We used two different *in vivo* models to test the role of IL-25. The first is a model of mild inflammation in the hippocampus obtained by causing anterograde axonal degeneration in the PP by injuring the entorhinal cortex (ECL). The second is a classical model of neuroinflammation, namely EAE.[47] Clinical beneficial effect of IL-25 gene therapy cannot be appreciated in the ECL model and was seen in EAE but only in the chronic model. We do not have an obvious explanation for the discrepancy between our findings and previous data on relapsing EAE,[9] other than that we use more adjuvant in our immunization protocol. From the pathological point of view, however, in ECL we found an increased number of $CD45^{high}CD11b^{+}$ cells in the lesion-reactive hippocampi. At the same time, we detected an overexpression of all M2 markers tested in IL-25HA-treated mice, analyzed by RT-PCR. This strongly suggests that IL-25 induces alternative activation *in vivo* in CNS-resident myeloid cells. As we have demonstrated in the past[37] and also in the present series of experiments (data not shown) that cytokines delivered through the ependymal route do not have any effect in the peripheral immune system, we have to assume that the main action of CNS-delivered IL-25 has been exerted on local microglia, rather than on already committed infiltrating macrophages.

In EAE, on the other hand, where the infiltration of the CNS by inflammatory cells is incomparably higher than in ECL,[49] we found a significant decrease of infiltrates in IL-25HA-treated mice, both by FACS and neuropathological analysis. This apparent discrepancy in the two models may be explained by the molecular analysis. When we analyzed the acute phase of EAE, characterized by massive infiltration of macrophages, we found that IL-25 gene

therapy is only able to inhibit pro-inflammatory cytokines, but not to induce an M2 profile. In the chronic phase of the disease, however, when the influx of myeloid cells from the blood stream is greatly reduced, anti-inflammatory cytokines such as IL-5 and IL-13, and the M2 marker Arg-1 are significantly increased by IL-25HA gene therapy. This may also explain why we do not find clinical benefit in RR-EAE, where recurrences are strongly inflammatory, not evolving to a chronic phase as in MOG-EAE.

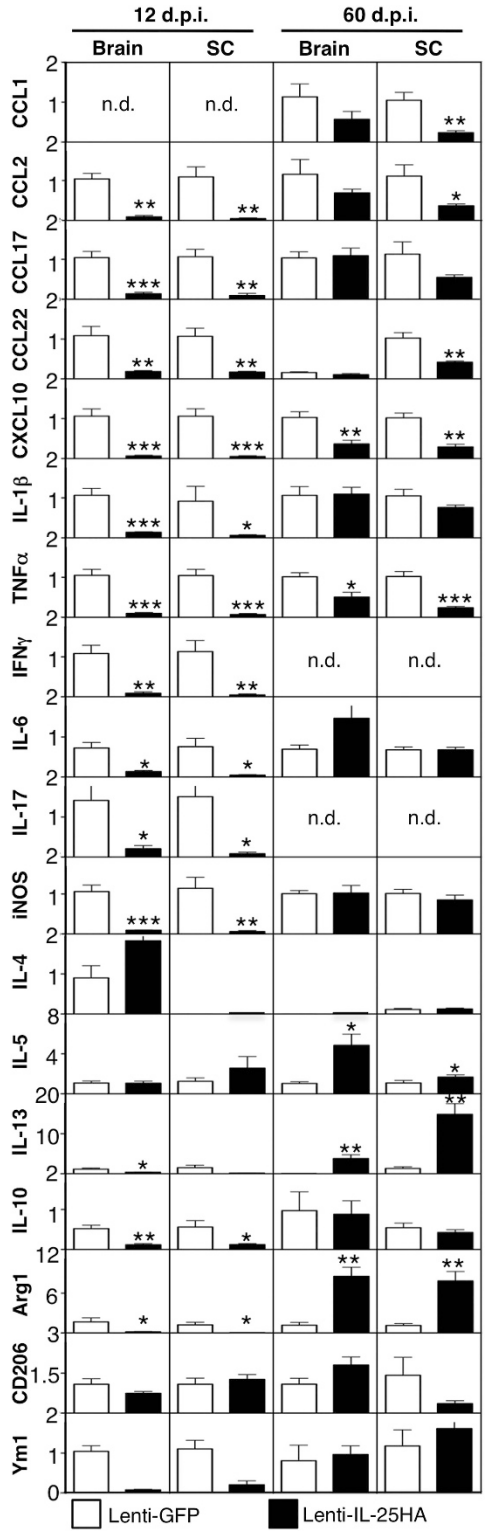

Inflammatory recurrences in RR-EAE cause swelling of the spinal cord that IL-25HA gene therapy is unable to counteract, not interfering with clinical course. The ability to modulate microglia, however, in the long range partially protects from tissue damage, as we show in Supplementary Figure 3. In both models, the tissue-protective effect of IL-25HA gene therapy might be related to the release of neurotrophic factor by modulated microglia. We found no induction, however, at the mRNA level, for GDNF, BDNF, IGF-I and TGFβ (data not shown). We cannot exclude that other neurotrophins are modulated and may have a role.

Why does IL-25 induce an anti-inflammatory profile in myeloid cells *in vivo*, while it is broadly inhibitory, both on M1 and M2 markers, *in vitro*? During the *in vitro* validation, we confirmed, for the first time by confocal microscopy, expression on the membrane of BM-derived macrophages of IL-17RB, the IL-25 receptor, that had previously been shown in mouse by flow cytometry.[13] We found that IL-25 induces Socs3, as was previously described,[15] and inhibits the transcription of pro- and anti-inflammatory cytokines in myeloid cells *in vitro*. We have examined the effect of IL-25 *in vitro* also on unfractionated splenocytes, obtaining the same results as in purified macrophages showing that the presence of third-party non-macrophage cells makes no difference. Similar *in vitro*/*in vivo* discrepancy on macrophages has been reported for IL-25 in a model of colitis.[14] It is tempting to speculate that myeloid cells display *in vivo*, but not *in vitro*, a phenotype prone to shift to M2 upon IL-25 stimulation. Further, the inflammatory microenvironment present in EAE may predispose microglia to this shift. This would fit very well with the idea of great plasticity of myeloid cells, keeping a certain functional phenotype by integrating a number of different inputs, most of which are certainly absent in conventional *in vitro* cultures. There may also be a time issue, as *in vivo* the time scale is much longer than in *in vitro* experiments, although we observed the M2 shift in ECL after only 48 h.

Microglia are believed to have a crucial role in the pathogenesis of several neurological disorders, but very little information is available on their functional phenotype during disease. We have shown in the present work one of the very few successful examples of *in vivo* CNS myeloid cell phenotype modulation with a selected cytokine, namely IL-25, by using our gene therapy approach targeting the CSF. We think this may constitute a useful tool to investigate the role of microglia-activation patterns during neurological disorders and, at the same time, a potential alternative therapeutic approach for CNS diseases in which microglia is believed to have a detrimental role.

Figure 7. IL-25 modulates inflammatory milieu during neuroinflammation. The expression of the following immune markers were analyzed by real-time (RT)-PCR analysis of brain and spinal cord tissues from IL-25HA-injected EAE mice ($n = 5$ at 12 d.p.i., $n = 4$ at 60 d.p.i.) and GFP-injected EAE mice ($n = 5$ at 12 d.p.i., $n = 4$ at 60 d.p.i.): CCL1, CCL2, CCL17, CCL22, CXCL10, IL-1β, TNF-α, IFNγ, IL-6, IL-17, iNOS, IL-4, IL-5, IL-13, IL-10, Arg-1, CD206 and Ym1. At 12 d.p.i., IL-25 inhibits most of the markers tested with the exception of IL-4, increased only in the brain of IL-25-injected EAE mice. At 60 d.p.i., IL-25 still downregulates the expression of several chemoattractant chemokines and pro-inflammatory cytokines, but it induces the expression of the anti-inflammatory cytokines IL-5 and IL-13, and of the M2 marker Arg-1; gene expression values were normalized on the glyceraldehyde-3-phosphate dehydrogenase housekeeping gene. Values for each target gene are reported on a single row. *Y* axis shows fold induction values. Interception between *y* and *x* axes occurs always at 0, although the value has been omitted to allow visualization of the maximum value of the lower graph. Lenti-GFP = GFP-lentivirus-injected mice (open bars), Lenti-IL-25HA = IL-25HA-lentivirus-injected mice (closed bars), ND = not detectable; SC = spinal cord. Column bars represent mean fold induction with s.e.m.; $^{*}P < 0.05$, $^{**}P < 0.01$, $^{***}P < 0.001$. One asterisk significance is lost after Bonferroni's correction for multiple comparisons.

MATERIALS AND METHODS

Generation of mouse IL-25-expressing lentivirus

Mouse IL-25 (mIL-25) was cloned from RNA of naive SJL mice. RNA was extracted in Trizol (Invitrogen, Paisley, UK) and complementary DNA (cDNA) synthesis was performed using ThermoScript RT-PCR System (Invitrogen) with a specific RT primer: 5′-TACAC CTGCCCCTCTCTCCC-3′. mIL-25 cDNA was amplified by PCR using GoTaq Flexi DNA Polymerase according to the methods (Promega, Madison, WI, USA), forward primer 5′-GGGATATCACCATGTACCAGGCTGTTGCATTCTTGGC-3′ and reverse primer 5′-CCCGTCTCAGGTAAGCCATGACCCGGGGCCGCAC-3′. The coding sequence for HA epitope tag was inserted in a polylinker by ligation of four oligos. pol1: 5′-ATCAACCGT CTCATACCCATACGACGTGC-3′; pol2: 5′-CAGACTACGC ATAGG-3′; pol3: 5′-TCGACCTATGCGTAGTCTGGCACG-3′; and pol4: 5′-TCG TATGGGTATG AGACGGTTGAT-3′. Then mIL-25 cDNA was linked to HA-tag by a step cloning into pcDNA3.1 plasmid. A third-generation lentivirus expressing mIL-25HA was generated cloning the mIL-25HA cDNA in the backbone of a p277 lentiviral transfer vector and producing a lentivirus as previously described.[50] A GFP-expressing lentivirus was also produced to be used as negative control in all the *in vitro* and *in vivo* experiments.

IL-25 *in vitro* production

HEK293T cells were grown in Iscove Modified Dulbecco Medium supplemented with 10% of fetal bovine serum (FBS), 2 mM ultra-glutamin and 100 U ml penicillin/streptomycin (Lonza, Braine-l'Alleud, Belgium). Cells were seeded at 50 000 per well in a 6-well plate (Corning Incorporated Life Sciences, Lowell, MA, USA) and, 24 h later, infected by IL-25HA-expressing or GFP-expressing lentivirus (multiplicity of infection = 5). After 48 h, IL-25HA or GFP-conditioned medium were collected and stored at − 80 °C for western blot analysis or BM-derived macrophages *in vitro* functionality assay. IL-25HA or GFP-infected cells were lysed with a scraper in 300 µl of Lysis Buffer (150 mM NaCl, 1% Triton-X-100, 50 mM Tris HCl pH 8.0) (powders from Sigma, St Louis, MO, USA) for western blot analysis.

BM-derived macrophages *in vitro* culture

Macrophages were isolated from BM's flushing and cultured with macrophage-colony stimulating factor (100 ng ml^{-1}, Miltenyi Biotec GmbH, Bergisch Gladbach, Germany) in α-Minimum Essential Medium (MEM) (Invitrogen) for 7 days. The purity of BM-macrophages' cultures was confirmed by FACS using CD11b (1:100, BD Biosciences, Mountain View, CA, USA) and F4/80 (1:100, BioLegend, San Diego, CA, USA) antibodies. Differentiated macrophages were cultured on coverslip glasses in α-MEM medium (Invitrogen) for 48 h for immunofluorescence studies.

To analyze phosphorylation of p38 protein, differentiated macrophages were incubated with IL-25HA or GFP-conditioned media (in a ratio 1:1, 1:0.5, 1:0.25 to α-MEM) for 30 min. rIL-25 (25–50 ng ml^{-1}, R&D Systems, Minneapolis, MN, USA) was used as positive control. Then cells were lysed with a scraper in 100 µl of Lysis Buffer (150 mM NaCl, 1% Triton-X-100, 50 mM Tris HCl pH 8.0) (powders from Sigma) for western blot analysis.

For RT-PCR analysis, differentiated macrophages were cultured with IL-25HA or GFP-conditioned media in a ratio 1:1 to α-MEM for 48 h. rIL-25 (50 ng ml^{-1}, R&D Systems) was used as positive control. Then cells were lysed in Trizol (Invitrogen) for RNA extraction.

Immunofluorence studies

BM-derived macrophages were post-fixed in paraformaldehyde (PFA) 4% for 10 min and incubated in 5% FBS-PBS1X for 1 h, to block any nonspecific binding site. Primary anti-IL-17rb (1:20, R&D Systems) and anti-F4/80 (1:200, Abcam, Cambridge, MA, USA) antibodies were used to reveal IL-17rb and F4/80 on macrophages. Alexa-fluor secondary antibodies (546 for IL-17rb and 488 for F4/80) from Molecular Probes (Invitrogen) were used.

Sections from lesion-reactive hippocampi of GFP-injected or IL-25HA-injected mice were post-fixed in PFA 4% for 10 min and then incubated in 5% FBS-PBS1X for 1 h, to block any nonspecific binding site. Primary anti-HA (1:1,000, eBioscience, San Diego, CA, USA), anti-Iba1 (1:400, Wako Chemicals USA Inc., Richmond, VA, USA) and anti-CD206 (1:200, BD Biosciences) antibodies were used to stain infected epedymal cells, myeloid cells and IL-17rb, respectively. Alexa-fluor secondary antibodies (1:200; 488 for HA or IL-17rb, 546 for CD206) from Molecular Probes (Invitrogen) were used.

In all the experiments, nuclei were stained with 4′6-diamidino-2-phenylindole (1:25 000; Roche Diagnostics Spa, Monza, Italy). Staining omitting the primary antibodies were used as negative control. A Leica (Leica Microsystems, Milano, Italy) confocal microscopy for the acquisitions of pictures was used.

Western Blot

Kit BCA Protein Assay (Thermoscientific, Waltham, MA, USA) was used to quantify proteins in cells' lysates (HEK293T cells, BM-macrophages). Twenty micrograms of proteins from IL-25HA or GFP-infected HEK293T and IL-25HA or GFP-treated BM-macrophages were subjected to SDS (Sigma)—12% PAGE before blotting onto a polyvinylidene difluoride membrane (Whatman, GE Healthcare, Waukesha, WI, USA). Membranes were blocked with 5% skimmed milk in Tris-buffered saline with 0.05% Tween 20 (pH 7.6) (Sigma) for 1 h at room temperature, and probed with primary anti-HA-tag (1:20, eBioscience), anti-βactin (1:30 000, Sigma), anti-p38 and anti-p38 (1:1000; phospho T180 + Y182) monoclonal antibody (Abcam) for 2 h at room temperature. Membranes were then incubated with secondary peroxidase-conjugated AffiniPure anti-rabbit or anti-mouse IgG (H + L) antibodies (1:10 000; Jackson Immuno Reaserch, Suffolk, UK) for 1 h at room temperature. Antibody–antigen complexes were then detected using ECL IMMOBILON WESTERN Chemiluminescent HRP-substrate detection system (Millipore, Billerica, MA, USA) according to the manufacturer's instructions.

Mice

For ECL mouse model 8-week-old C57BL/6 wild-type mice were purchased from Taconic (Taconic Europe, Lille Skensved, Denmark). For EAE mouse model 8-week-old C57Bl/6 and SJL wild-type female mice were obtained from Charles River (Calco, Italy). Mice were provided with food and water *ad libitum* and were housed under pathogen-free conditions with a constant light/dark cycle. All procedures involving animals were performed according to the guidelines of the National Danish Animal Research Committee and to the animal protocol guidelines prescribed by the Institutional Animal Care and Use Committee (IACUC #331) at San Raffaele Scientific Institute (Milan, Italy).

Intracisterna magna injection

Intrathecal injection of lentivirus were performed as described previously[38] at the desired time point. A 30-gauge needle attached to a Hamilton syringe were inserted into the intrathecal space of the *cisterna magna* of anesthetized mice. IL-25HA-expressing or GFP-expressing lentiviruses (10 µl) in sterile phosphate-buffered saline (10^9 PFU ml^{-1}) were injected over 30 s.

IL-25 gene therapy of ECL mouse model

C57BL/6 mice received an *intra cisterna magna* (i.c.) injection of IL-25HA-expressing or GFP-expressing lentivirus (10 µl, 10^9 ml^{-1}) 5 days before perfoming ECL. Under anesthesia, mice were placed in a Kopf stereotactic apparatus (Kopf Instruments, Tujunga, CA, USA) and a burr hole was drilled in the skull 1.9 mm lateral to lambda and 0.3 mm caudal to the lambdoid suture. The nosebar was set at 3 mm. A wire knife (Kopf Instruments) was inserted at an angle of 15 ° rostrally and 10 ° laterally, and 3.4 mm ventral to the meninges, the knife was unfolded and the entorhinodentate PP projection was sectioned by retracting the knife 3.2 mm.[44] Mice were killed 48 h post surgical lesion for real-time PCR, FACS or histological analysis.

IL-25 gene therapy of EAE mouse model

Chronic EAE was induced in female C57BL/6 mice, by subcutaneus with 300 µl of 200 µg per mouse of $MOG_{35–55}$ (Espikem, Florence, Italy) in IFA (Sigma) supplemented with 8 mg ml^{-1} *Mycobacterium tuberculosis* (strain H37Ra; Difco, Lawrence, KS, USA). *Pertussis toxin* (500 ng, List Biological Laboratories, Campbell, CA, USA) was injected intraperitoneally on the day of the immunization and again 2 days later, as described. IL-25HA-expressing lentivirus or GFP-expressing lentivirus were injected in the cisterna magna (i.c.) of the mice at fifth d.p.i.

RR-EAE was induced in female SJL/j mice, by two subcutaneus injections, 7 days apart, into both flanks with 100 µl of an emulsion containing 200 µg per mouse of $PLP_{139–151}$ (Espikem) and 8 mg ml^{-1} of heat-killed *M. tuberculosis* in IFA. In addition, mice received four intraperitoneal injections of 500 ng of *Pertussis toxin* on the day of immunization and 24 h later, as described.[51,52] IL-25HA-expressing lentivirus or GFP-expressing lentivirus were injected i.c. at twelth or eighteenth d.p.i.

Mice were weighed and scored for clinical signs daily up to the day of culling. Clinical assessment of EAE was performed according to the following scoring criteria: 0 = healthy; 1 = limp tail; 2 = ataxia and/or paresis of hindlimbs; 3 = paralysis of hindlimbs and/or paresis of forelimbs; 4 = tetraparalysis; and 5 = moribund or death.

Chronic-EAE mice were killed at twelth or sixtieth d.p.i for real-time PCR, FACS and histological analysis. RR-EAE mice were killed at fiftieth d.p.i. for histological analysis.

ELISA assay for mIL-25

mIL-25HA was measured in supernatants and lysates of infected cells or CSFs (withdrawn from mice cisterna magna by capillarity) or brain homogenates from IL-25-injected EAE mice, using DUOset ELISA mouse IL-17-E (R&D Systems).

Preparation of CNS mononuclear cells

For ECL and EAE experiments, mice were deeply anesthetized and perfused transcardially with cold phosphate-buffered saline at the indicated time point. For ECL, brains were removed, and controlateral and lesion-reactive (ipsilateral) hippocampi were dissected out and homogenized through a 70 μm cell strainer (BD Falcon, Mountain View, CA, USA) in HBSS (Invitrogen). Mononuclear cells were then washed with cold PBS1X three times and collected by centrifugation for flow cytometric staining.

For EAE, brains and the spinal cords were dissected out at the desired time point, removed and homogenized through a 70-μm cell strainer in HBSS. Mononuclear cells were isolated by 30/37/70% percoll (GE Healthcare) gradient centrifugation and collection of mononuclear cells from the 37/70% interphase.

Abs and FACS analysis

For ECL experiments, cells were stained with the following monoclonal antibodies (all from BD Biosciences): PE-conjugated anti-CD45 (1:400), PerCP-conjugated anti-CD11b (1:100) and allophycocyanin-conjugated anti-TCR (1:200) antibodies to detect microglia/macrophages or T cells, respectively.[53,54]

For EAE experiments, cells were stained with the following monoclonal antibodies (all from BD Biosciences): APC-conjugated anti-CD45 (1:100), APC-Cy7-conjugated anti-CD11b (1:100) and PE-Cy7- conjugated anti-CD3e (1:100) antibodies to detect microglia/macrophages or T cells, respectively.

5000 BD Calibrate Beads were added for sample. Both ECL- and EAE-derived cells were all collected on a FACSCanto machine (BD Biosciences) and analyzed using FCSexpress software (De Novo Software, Los Angeles, CA, USA).

Histological evaluation

At least four EAE mice per group were perfused at sixtieth d.p.i. through the left cardiac ventricle with saline, plus EDTA 0.5 M for 10 min followed by fixation with cold 4% PFA (Sigma) in 0.1 M phosphate buffer (pH 7.4). Subsequently, spinal cords and brains from EAE mice were carefully dissected out and post-fixed in 4% PFA overnight and processed for cryogenic embedding. The quantification of neurological damage in EAE mice was performed via histological analysis of 10 μm frozen CNS sections of control or IL-25HA-injected or GFP-injected EAE mice. Three different staining were used to detect inflammatory infiltrates (Hematoxylin and Eosin), demyelination (Luxol fast blue) and axonal damage (Bielshowsky). Neuropathological findings were quantified on an average of 10 complete cross-sections of spinal cord per mouse taken at eight different levels of the spinal cord. The number of perivascular inflammatory infiltrates were calculated and expressed as the numbers of inflammatory infiltrates per mm^2, demyelinated areas and axonal loss were expressed as percentage of damaged area.

Immunohistochemistry for HA-tag (anti-HA antibody 1:20, eBioscience) was performed to characterize mIL-25HA-positive cells in the lentivirus-infected EAE brain. Labeling was revealed with an appropriate biotin-labeled secondary antibody (1:500, Amersham, Airlington Heights, IL, USA) and developed with the ABC kit (Vector Laboratories, Burlingame, CA, USA) followed by either liquid DAB Substrate Chromogen System (DAKO, Glostrup, Denmark) or Peroxidase Substrate Kit TMB (Vector Laboratories). An Olympus microscope (Olympus, Segrate, Italy) for the acquisitions of pictures was used.

RT-PCR analysis

RT-PCR analyses were perfomed for *in vitro* BM-derived macrophages assay and for IL-25 gene therapy studies of ECL model or EAE model. Briefly, RNA was extracted in Trizol (Invitrogen). Residual DNA was removed by treatment with 1 U DNase per 1 μg RNA (RQ1 RNase-free DNase, Promega) at 37 °C for 30 min. cDNA synthesis from 3–5 μg total RNA was performed using Ready-To-Go You-Prime First-Strand Beads (Amersham) and Random Hexamer (New England Biolabs, Ipswich, MA, USA) according to the manufacturer's instructions. *Arg-1* (Mm00475988_m1), *CCL1* (Mm00441236_m1), *CCL2* (Mm00441242_m1), *CCL17* (Mm00516136_m1), *CCL22* (Mm00436439_m1), *CD206* (Mm00485148_m1), *CXCL10* (Mm00445235_m1), *IFNγ* (Mm01168134_m1), *IL-1β* (Mm01336189_m1), *IL-4* (Mm00445259_m1), *IL-5* (Mm00439646_m1), *IL-6* (Mm00446190_m1), *IL-10* (Mm00439616_m1), *IL-13* (Mm00434204_m1), *IL-17* (Mm00439618_m1), *IL-25* (Mm00499822_m1), *iNOS* (Mm00440502_m1), *Socs3* (Mm00545913_s1), *TNF-α* (Mm00443258_m1) and *Ym1* (Mm00657889_mH) mRNA levels were measured by real-time RT-PCR (Applied Biosystem, Invitrogen). The $2^{-\Delta\Delta CT}$ method was used to calculate relative changes in gene expression.[55]

Statistical analysis

Statistical evaluations of RT-PCR data, ELISA assay, FACS data, EAE score and immunohistochemical analyses results were expressed as mean ± s.e.m. Results were analyzed using the unpaired Student's *t*-test and Mann–Whitney *U*-test for samples with unknown and potentially disparate variances. Analyses were performed using the Prism V5.0a software (Graph-Pad, San Diego, CA, USA). Statistical significance was accepted when $^{*}P<0.05$, $^{**}P<0.01$, $^{***}P<0.001$.

CONFLICT OF INTEREST

The authors declare no conflict of interest.

ACKNOWLEDGEMENTS

We are grateful to P Brown for helpful discussion; to Prof. L Naldini for providing the lentiviral backbone; to A Gatta, E Butti, D Dræby, M Rytz Hansen and P Nyborg Nielsen for technical help.

REFERENCES

1 Moseley TA, Haudenschild DR, Rose L, Reddi AH. Interleukin-17 family and IL-17 receptors. *Cytokine Growth Factor Rev* 2003; **14**: 155–174.
2 Ikeda K, Nakajima H, Suzuki K, Kagami S, Hirose K, Suto A *et al.* Mast cells produce interleukin-25 upon Fc epsilon RI-mediated activation. *Blood* 2003; **101**: 3594–3596.
3 Kang CM, Jang AS, Ahn MH, Shin JA, Kim JH, Choi YS *et al.* Interleukin-25 and interleukin-13 production by alveolar macrophages in response to particles. *Am J Respir Cell Mol Biol* 2005; **33**: 290–296.
4 Wang YH, Angkasekwinai P, Lu N, Voo KS, Arima K, Hanabuchi S *et al.* IL-25 augments type 2 immune responses by enhancing the expansion and functions of TSLP-DC-activated Th2 memory cells. *J Exp Med* 2007; **204**: 1837–1847.
5 Wong CK, Cheung PF, Ip WK, Lam CW. Interleukin-25-induced chemokines and interleukin-6 release from eosinophils is mediated by p38 mitogen-activated protein kinase, c-Jun N-terminal kinase, and nuclear factor-kappaB. *Am J Respir Cell Mol Biol* 2005; **33**: 186–194.
6 Zaph C, Du Y, Saenz SA, Nair MG, Perrigoue JG, Taylor BC *et al.* Commensal-dependent expression of IL-25 regulates the IL-23-IL-17 axis in the intestine. *J Exp Med* 2008; **205**: 2191–2198.
7 Angkasekwinai P, Park H, Wang YH, Chang SH, Corry DB, Liu YJ *et al.* Interleukin 25 promotes the initiation of proallergic type 2 responses. *J Exp Med* 2007; **204**: 1509–1517.
8 Fort MM, Cheung J, Yen D, Li J, Zurawski SM, Lo S *et al.* IL-25 induces IL-4, IL-5, and IL-13 and Th2-associated pathologies *in vivo*. *Immunity* 2001; **15**: 985–995.
9 Kleinschek MA, Owyang AM, Joyce-Shaikh B, Langrish CL, Chen Y, Gorman DM *et al.* IL-25 regulates Th17 function in autoimmune inflammation. *J Exp Med* 2007; **204**: 161–170.
10 Tamachi T, Maezawa Y, Ikeda K, Kagami S, Hatano M, Seto Y *et al.* IL-25 enhances allergic airway inflammation by amplifying a TH2 cell-dependent pathway in mice. *J Allergy Clin Immunol* 2006; **118**: 606–614.
11 Cao Q, Wang C, Zheng D, Wang Y, Lee VW, Wang YM *et al.* IL-25 induces M2 macrophages and reduces renal injury in proteinuric kidney disease. *J Am Soc Nephrol* 2011; **22**: 1229–1239.
12 Caruso R, Stolfi C, De Nitto D, Pallone F, Monteleone G. The dual role of interleukin-25 in the control of immune-mediated pathologies. *Curr Mol Med* 2011; **11**: 26–30.
13 Dolgachev V, Petersen BC, Budelsky AL, Berlin AA, Lukacs NW. Pulmonary IL-17E (IL-25) production and IL-17RB+ myeloid cell-derived Th2 cytokine production are dependent upon stem cell factor-induced responses during chronic allergic pulmonary disease. *J Immunol* 2009; **183**: 5705–5715.

14 Rizzo A, Monteleone I, Fina D, Stolfi C, Caruso R, Fantini MC *et al*. Inhibition of colitis by IL-25 associates with induction of alternatively activated macrophages. *Inflamm Bowel Dis* 2011; **18**: 449–459.
15 Caruso R, Stolfi C, Sarra M, Rizzo A, Fantini MC, Pallone F *et al*. Inhibition of monocyte-derived inflammatory cytokines by IL-25 occurs via p38 Map kinase-dependent induction of Socs-3. *Blood* 2009; **113**: 3512–3519.
16 Stolfi C, Caruso R, Franze E, Sarra M, De Nitto D, Rizzo A *et al*. Interleukin-25 fails to activate STAT6 and induce alternatively activated macrophages. *Immunology* 2011; **132**: 66–77.
17 Biswas SK, Mantovani A. Macrophage plasticity and interaction with lymphocyte subsets: cancer as a paradigm. *Nat Immunol* 2010; **11**: 889–896.
18 Gordon S, Martinez FO. Alternative activation of macrophages: mechanism and functions. *Immunity* 2010; **32**: 593–604.
19 Mantovani A, Sozzani S, Locati M, Allavena P, Sica A. Macrophage polarization: tumor-associated macrophages as a paradigm for polarized M2 mononuclear phagocytes. *Trends Immunol* 2002; **23**: 549–555.
20 Adams DO, Hamilton TA. The cell biology of macrophage activation. *Annu Rev Immunol* 1984; **2**: 283–318.
21 Hamilton T. Molecular basis of macrophage activation: from gene expression to phenotypic diversity. In: Lewis BBCE (ed). *In The Macrophage*. 2nd edn. Oxford University Press: Oxford, UK, 2002.
22 Kigerl KA, Gensel JC, Ankeny DP, Alexander JK, Donnelly DJ, Popovich PG. Identification of two distinct macrophage subsets with divergent effects causing either neurotoxicity or regeneration in the injured mouse spinal cord. *J Neurosci* 2009; **29**: 13435–13444.
23 Mantovani A, Allavena P, Sica A, Balkwill F. Cancer-related inflammation. *Nature* 2008; **454**: 436–444.
24 Mosser DM, Edwards JP. Exploring the full spectrum of macrophage activation. *Nat Rev Immunol* 2008; **8**: 958–969.
25 Stein M, Keshav S, Harris N, Gordon S. Interleukin 4 potently enhances murine macrophage mannose receptor activity: a marker of alternative immunologic macrophage activation. *J Exp Med* 1992; **176**: 287–292.
26 Lassmann H, Bruck W, Lucchinetti CF. The immunopathology of multiple sclerosis: an overview. *Brain Pathol* 2007; **17**: 210–218.
27 Fenn AM, Henry CJ, Huang Y, Dugan A, Godbout JP. Lipopolysaccharide-induced interleukin (IL)-4 receptor-alpha expression and corresponding sensitivity to the M2 promoting effects of IL-4 are impaired in microglia of aged mice. *Brain Behav Immun* 2012; **26**: 776–777.
28 Henkel JS, Beers DR, Zhao W, Appel SH. Microglia in ALS: the good, the bad, and the resting. *J Neuroimmune Pharmacol* 2009; **4**: 389–398.
29 Michelucci A, Heurtaux T, Grandbarbe L, Morga E, Heuschling P. Characterization of the microglial phenotype under specific pro-inflammatory and anti-inflammatory conditions: effects of oligomeric and fibrillar amyloid-beta. *J Neuroimmunol* 2009; **210**: 3–12.
30 Salemi J, Obregon DF, Cobb A, Reed S, Sadic E, Jin J *et al*. Flipping the switches: CD40 and CD45 modulation of microglial activation states in HIV associated dementia (HAD). *Mol Neurodegener* 2011; **6**: 3.
31 Johnston H, Boutin H, Allan SM. Assessing the contribution of inflammation in models of Alzheimer's disease. *Biochem Soc Trans* 2011; **39**: 886–890.
32 Perry VH, Nicoll JA, Holmes C. Microglia in neurodegenerative disease. *Nat Rev Neurol* 2010; **6**: 193–201.
33 Polazzi E, Monti B. Microglia and neuroprotection: from *in vitro* studies to therapeutic applications. *Prog Neurobiol* 2010; **92**: 293–315.
34 Schwartz M, Butovsky O, Bruck W, Hanisch UK. Microglial phenotype: is the commitment reversible? *Trends Neurosci* 2006; **29**: 68–74.
35 Zhang Z, Zhang ZY, Schittenhelm J, Wu Y, Meyermann R, Schluesener HJ. Parenchymal accumulation of CD163+ macrophages/microglia in multiple sclerosis brains. *J Neuroimmunol* 2011; **237**: 73–79.
36 Martino G, Furlan R, Comi G, Adorini L. The ependymal route to the CNS: an emerging gene-therapy approach for MS. *Trends Immunol* 2001; **22**: 483–490.
37 Butti E, Bergami A, Recchia A, Brambilla E, Del Carro U, Amadio S *et al*. IL4 gene delivery to the CNS recruits regulatory T cells and induces clinical recovery in mouse models of multiple sclerosis. *Gene Therapy* 2008; **15**: 504–515.
38 Furlan R, Brambilla E, Ruffini F, Poliani PL, Bergami A, Marconi PC *et al*. Intrathecal delivery of IFN-gamma protects C57BL/6 mice from chronic-progressive experimental autoimmune encephalomyelitis by increasing apoptosis of central nervous system-infiltrating lymphocytes. *J Immunol* 2001; **167**: 1821–1829.
39 Furlan R, Pluchino S, Marconi PC, Martino G. Cytokine gene delivery into the central nervous system using intrathecally injected nonreplicative viral vectors. *Methods Mol Biol* 2003; **215**: 279–289.
40 Furlan R, Poliani PL, Galbiati F, Bergami A, Grimaldi LM, Comi G *et al*. Central nervous system delivery of interleukin 4 by a nonreplicative herpes simplex type 1 viral vector ameliorates autoimmune demyelination. *Hum Gene Ther* 1998; **9**: 2605–2617.
41 Millward JM, Caruso M, Campbell IL, Gauldie J, Owens T. IFN-gamma-induced chemokines synergize with pertussis toxin to promote T cell entry to the central nervous system. *J Immunol* 2007; **178**: 8175–8182.
42 Millward JM, Lobner M, Wheeler RD, Owens T. Inflammation in the central nervous system and Th17 responses are inhibited by IFN-gamma-Induced IL-18 binding protein. *J Immunol* 2010; **185**: 2458–2466.
43 Jensen MB, Hegelund IV, Poulsen FR, Owens T, Zimmer J, Finsen B. Microglial reactivity correlates to the density and the myelination of the anterogradely degenerating axons and terminals following perforant path denervation of the mouse fascia dentata. *Neuroscience* 1999; **93**: 507–518.
44 Khorooshi R, Babcock AA, Owens T. NF-kappaB-driven STAT2 and CCL2 expression in astrocytes in response to brain injury. *J Immunol* 2008; **181**: 7284–7291.
45 Khorooshi R, Owens T. Injury-induced type I IFN signaling regulates inflammatory responses in the central nervous system. *J Immunol* 2010; **185**: 1258–1264.
46 Wirenfeldt M, Dissing-Olesen L, Anne Babcock A, Nielsen M, Meldgaard M, Zimmer J *et al*. Population control of resident and immigrant microglia by mitosis and apoptosis. *Am J Pathol* 2007; **171**: 617–631.
47 Furlan R, Cuomo C, Martino G. Animal models of multiple sclerosis. *Methods Mol Biol* 2009; **549**: 157–173.
48 Rickel EA, Siegel LA, Yoon BR, Rottman JB, Kugler DG, Swart DA *et al*. Identification of functional roles for both IL-17RB and IL-17RA in mediating IL-25-induced activities. *J Immunol* 2008; **181**: 4299–4310.
49 Ajami B, Bennett JL, Krieger C, McNagny KM, Rossi FM. Infiltrating monocytes trigger EAE progression, but do not contribute to the resident microglia pool. *Nat Neurosci* 2011; **14**: 1142–1149.
50 Follenzi A, Ailles LE, Bakovic S, Geuna M, Naldini L. Gene transfer by lentiviral vectors is limited by nuclear translocation and rescued by HIV-1 pol sequences. *Nat Genet* 2000; **25**: 217–222.
51 Amadio S, Pluchino S, Brini E, Morana P, Guerriero R, Boneschi FM *et al*. Motor evoked potentials in a mouse model of chronic multiple sclerosis. *Muscle Nerve* 2006; **33**: 265–273.
52 Pluchino S, Quattrini A, Brambilla E, Gritti A, Salani G, Dina G *et al*. Injection of adult neurospheres induces recovery in a chronic model of multiple sclerosis. *Nature* 2003; **422**: 688–694.
53 Babcock AA, Kuziel WA, Rivest S, Owens T. Chemokine expression by glial cells directs leukocytes to sites of axonal injury in the CNS. *J Neurosci* 2003; **23**: 7922–7930.
54 Babcock AA, Wirenfeldt M, Holm T, Nielsen HH, Dissing-Olesen L, Toft-Hansen H *et al*. Toll-like receptor 2 signaling in response to brain injury: an innate bridge to neuroinflammation. *J Neurosci* 2006; **26**: 12826–12837.
55 Livak KJ, Schmittgen TD. Analysis of relative gene expression data using real-time quantitative PCR and the 2(-Delta Delta C(T)) Method. *Methods* 2001; **25**: 402–408.

Supplementary Information accompanies the paper on Gene Therapy website (http://www.nature.com/gt)